

The Pennsylvania State University
The Graduate School

**MECHANISM OF HISTONE EXCHANGE BY INO80
CHROMATIN REMODELER**

A Thesis in
Chemistry
by
Sirong Lin

© 2019 Sirong Lin

Submitted in Partial Fulfillment
of the Requirements
for the Degree of

Master of Science

August 2019

The thesis of Sirong Lin was reviewed and approved* by the following:

Tae-Hee Lee

Associate Professor of Chemistry and the Huck Institute of the Life Sciences

Thesis Adviser

Joseph Cotruvo

Assistant Professor of Chemistry

Louis Martarano Career Development Professor

Xin Zhang

Assistant Professor of Chemistry

Assistant Professor of Biochemistry and Molecular Biology

Paul Berg Early Career Professorship in the Eberly College of Science

Philip C. Bevilacqua

Distinguished Professor of Chemistry and Biochemistry and Molecular Biology

Head of the Department of Chemistry

*Signatures are on file in the Graduate school.

Abstract

The nucleosome, made of an octameric histone protein core wrapped around by ~147 base-pair double-stranded DNA, is the fundamental gene-packing unit in eukaryotes. The structure of the nucleosome is flexible, which is the physical basis of dynamic gene regulation mechanisms. Various biochemical signals are involved in regulating the positions of nucleosomes or altering the composition of histone cores, which are often mediated by chromatin remodelers. A chromatin remodeler INO80 slides nucleosomes and exchanges histone H2A.Z with H2A, which have been associated with transcription activation and active transcription. H2A.Z is enriched in the promoter proximal nucleosomes that can potentially act as physical barriers to help maintain genome integrity. The barriers would be lowered when H2A.Z is replaced with H2A, which would subsequently catalyze gene activation. One of the prevailing hypotheses has been that INO80 carries out this function although its molecular mechanism remains nearly completely unknown. Here I present the mechanism of how INO80 exchanges H2A.Z with H2A based on three-color single-molecule FRET measurements. According to the mechanism, INO80 carries a histone H2A-H2B dimer, unwraps DNA while it translocates along the nucleosome, and exchanges H2A.Z-H2B with H2A-H2B. I also propose that the substrate specificity of the dimer exchange reaction is due to potential preferential binding of INO80 to H2A.Z-H2B over H2A-H2B.

Table of Contents

List of Tables.....	26
List of Figures.....	10
Chapter 1. Introduction.....	5
1.1 The Nucleosome core particle.....	5
1.2 Chromatin remodelers.....	5
1.3 Single -molecule fluorescence resonance energy transfer (smFRET).....	6
Chapter 2. Materials and Methods.....	6
2.1 Materials.....	7
2.1.1 Media.....	7
2.1.2 Purification buffers.....	7
2.1.3 Gel buffers.....	7
2.1.4 Other buffer.....	8
2.1.5 Kits.....	8
2.1.6 Cells and proteins.....	8
2.1.7 Slides & Filters	8
2.2 Preparation of proteins and nucleosomes.....	8
2.2.1 Histone expression and purification.....	8
2.2.2 Histone refolding and purification.....	9
2.2.3 Dye labeling on DNA.....	9
2.2.4 Dye labeling of histone protein.....	9
2.2.5 DNA construction.....	10
2.2.6 Nucleosome reconstitution.....	10
2.2.7 SDS gel electrophoresis.....	10
2.2.8 Native gel electrophoresis.....	10
2.3 Single-molecule FRET measurements.....	11
2.3.1 Surface functionalization.....	12
2.3.2 preparation of sample chamber.....	14

Chapter 3. Mechanism of dimer exchange reaction by INO80.....	15
3.1 Introduction.....	15
3.2 Materials and Methods.....	16
3.3 Results.....	17
3.4 Discussion.....	27
References.....	30

Chapter 1. Introduction

1.1 The Nucleosome core particle

The nucleosome is the fundamental packing unit of DNA in eukaryotes. A nucleosome core particle contains ~147 base pairs (bp) of DNA wrapped in 1.67 left-handed superhelical turns around a histone octamer made of two molecules of H2A, H2B, H3, and H4.¹ The H2A-H2B heterodimer (A-dimer) and the (H3-H4)₂ tetramer are the minimal units of histone that is stable under a physiological buffer condition.

The dynamic structure of the nucleosome plays crucial roles in gene regulation. The thermodynamic stability of the nucleosome structure is mainly due to the strong electrostatic interactions between the positively charged histone core, and the negatively charged DNA.¹ Nucleosomes impose physical barriers to nuclear processes involving enzymes that translocate along DNA.^{1,2,3} Variations in the nucleosomal barriers are implemented by post-translational modifications of histone proteins and their variants. For example, acetylation at histone H3K56 lowers the entry barrier to the nucleosome and H2A.Z that replaces H2A in the +1/-1 nucleosome to a gene promoter helps keep genome integrity possibly by imposing higher physical barriers.^{1,2,3} Despite the crucial roles of these regulatory signals, how they affect the structure and structural dynamics of the nucleosome and how such effects would contribute to gene regulation remains poorly understood. Elucidating these effects and their implications in gene regulation will help us better understand the molecular mechanisms of gene regulation.

1.2 Chromatin remodelers

Chromatin remodeling is involved in various gene regulatory activities. There are mainly four families of chromatin remodelers in eukaryotes: SWI/SNF, ISWI, NuRD/Mi-2/CHD, and INO80/SWR1.⁴ Chromatin remodelers can regulate gene expression by mediating interactions between histone and DNA. For example, +1 nucleosome to a gene promoter enriched with H2A.Z-H2B dimer (Z-dimer) is replaced with A-dimer by a chromatin remodeler INO80 in an ATP dependent manner during transcription activation.^{2,3} This exchange will alter the DNA-histone interactions in the nucleosome and subsequently various nucleosomal processes. INO80 (inositol requiring 80) has diverse functions, including but not limited to promoting transcriptional activation, DNA repair, and replication.^{4,5} INO80 contains more than 10 subunits, including the SWR1-related complexes. A split-ATPase domain with a long insertion present in the middle of the ATPase domain is the defining feature of SWR1 and INO80 family remodelers. The helicase-related (AAA-ATPase) Rvb1/2 proteins and one ARP (actin-related protein) protein preferentially bind to the split domain. Both yINO80 and ySWR1 complexes also contain actin and Arp4.⁴ SWR1 is unique in its ability to restructure the nucleosome by dissociating A-dimer and replacing them with Z-dimer. The mechanism of this exchange and the dimer specificity is unknown. Z-dimer (an alpha-C helix of H2A.Z) is specifically recognized by the Swr1-Z domain.⁶ Snf2 family ATPase complex Swr1 is required to recruit Htz1 in SWR-C/SWR1.⁷ INO80 is also a Snf2 ATPase. Another candidate for the

specificity is Arp5-Ies6 that is required for INO80 remodeling. It is also known that an A-dimer is in close proximity to Arp5-Ies6 in a nucleosome that is bound with INO80.⁸

1.3 Single-molecule fluorescence resonance energy transfer (smFRET)

Fluorescence is a photon-emitting process when an excited electron is falling back to a lower energy state. Spectroscopic methods based on fluorescence has been directly or indirectly applied to the detection and characterization of molecules.⁹ Fluorescence resonance energy transfer (FRET) has been utilized for fluorescence spectroscopy techniques. FRET takes place via a nonradioactive energy transfer mechanism through dipole-dipole coupling between two fluorophores: a donor and an acceptor. FRET efficiency is a function of many parameters including the distance between the donor and the acceptor. It can only occur if the distance is within approximately 10 nm.¹⁰ Therefore, time-resolved FRET efficiency measurements provide a means to probing the structural dynamics of a macromolecule. FRET efficiency depends mainly on three parameters:

1. The distance between the donor and the acceptor (The effective range for commercially available fluorophores are typically 1-10nm).¹¹
2. The overlap between the emission spectrum of the donor and the absorption spectrum of the acceptor. A larger overlap yields a higher FRET efficiency.
3. The relative orientation of the donor emission dipole moment to acceptor absorption dipole moment. The FRET efficiency becomes the maximum when the fluorophores are aligned parallel to each other.

The efficiency of FRET is inversely proportional to the 6th power of the distance between the donor and the acceptor. This unique property gives FRET an extreme sensitivity to a small change in the distance. Because it is capable of measuring distances on the sub-nanometer scale, FRET is frequently used in monitoring various biological macromolecular processes such as interaction between RNA-binding protein and RNA¹², and spontaneous DNA motion¹³ in a nucleosome. In general, the FRET efficiency is given by

$$E = 1/[1+(r/R_0)^6]$$

, where E is the FRET efficiency; r is the distance between the donor and the acceptor; R₀ is the Forster radius which is the distance between the donor and the acceptor when the FRET efficiency is 0.5 (50%). For a FRET pair Cy3/Cy5, the R₀ = 5.6 nm,¹⁴ resulting in 3 ~ 8 nm for the effective distance range for sensitive FRET measurements.

Chapter 2. Materials and Methods

2.1 Materials

All media were autoclaved before use. All buffers were prepared with Mili-Q deionized water (EMD millipore, Billerica, MA) and filtered with a filter device (Thermo Scientific “Nalgene” Rapid-Flow 90 mm Filter Unit).

2.1.1 Media

LB (lysogeny broth) (1L)—10g tryptone, 5g yeast extract, 10g NaCl

2xYT (1L)—16g Bactotryptone, 10g yeast extract, 5g NaCl

2.1.2 Purification buffers

Wash buffer—50mM Tris-HCl (pH 7.5), 100mM NaCl, 1mM EDTA, 1mM benzamidine

TW buffer—50mM Tris-HCl (pH 7.5), 100mM NaCl, 1mM EDTA, 1mM benzamidine, 1% Triton X-100

Unfolding buffer—20mM Tris-HCl (pH 7.5), 7 M Guanidium-HCl, 10mM DTT

SAU 1000—7M deionized Urea, 20mM sodium acetate, pH 5.2, 1M NaCl, 5mM BME, 1mM EDTA

SAU 600—7M deionized Urea, 20mM sodium acetate, pH 5.2, 600 mM NaCl, 5mM BME, 1mM EDTA

SAU 200—7M deionized Urea, 20mM sodium acetate, pH 5.2, 200mM NaCl, 5mM BME, 1mM EDTA

2.1.3 Gel buffers

SDS-PAGE 10x gel running buffer (1L)—248mM Trizma (30g), 1.92 M glycine (144g), 1% SDS (10g)

Native gel buffer— 0.5x TBE buffer

5x TBE buffer (pH 8)— 4g Trizma base, 27.5g boric acid, 0.5M EDTA (20mL)

TAE buffer—40mM Trizma base, 20mM acetic acid, 1mM EDTA

Coomassie Brilliant Blue R-250 Staining Solution (Bio-rad)

2.1.4 Other buffer

TE buffer— 10mM Tris-HCl (pH 8.0), 1mM EDTA

Labeling buffer (pH 7.0) – 10mM Tris-HCl (pH 7.0), 2 M NaCl, 1mM EDTA (pH 8), 1mM TCEP

Labeling buffer (pH 7.4) – 10mM Tris-HCl (pH 7.4), 2 M NaCl, 1mM EDTA (pH 8)

2.1.5 Kits

QIAprep Spin miniprep Kit (ID 27106)	Qiagen	Germany
QIAquick PCR purification kit (ID 28106)	Qiagen	Germany
QIAquick Gel Extraction kit (ID 28706)	Qiagen	Germany

2.1.6 Cells and proteins

BL21(DE3) cells	Thermo Fisher Scientific	Waltham, MA
BL21(DE3) pLysS cells	Thermo Fisher Scientific	Waltham, MA
T4 ligase	New England Biolabs	Ipswich, MA

2.1.7 Slides and filters

Quartz microscope Slides	G.Finkenbeiner	Waltham, MA
24mmx30mm Premium Cover Glass	Fisher Scientific	Pittsburgh, PA
Amicon ultra centrifugal filters	EMD millipore	Billerica, MA

2.2 Preparation of proteins and nucleosomes

2.2.1 Histone expression and purification

Xenopus laevis histone proteins were expressed and purified following a previously published protocol (ref) with slight modifications. Histones H2A, H2B, H3, and H4 were cloned into a pET3a vector. Then, the plasmids was transformed into BL21(DE3) pLysS cells (Thermo Fisher Scientific, Waltham, MA). After transformation, three colonies were picked. A 5mL LB medium containing 100 µg/ml ampicillin was inoculated with cells from each colony and was shaken for 16h at 225 rpm at 37 °C. Each culture was delivered to a 1L 2x YT medium containing 100 µg/ml ampicillin that was shaken at 225 rpm at 37 °C until OD₆₀₀ reached ~0.6. Histone expression was subsequently induced by adding IPTG to a final concentration of 0.2 mM. After 3 hours of induction, cells were harvested by centrifugation at 5,000 rpm for 20 min at room temperature. The cell pellet was

resuspended in 20 ml of the wash buffer (0.05 M Tris-HCl pH 7.5, 0.1 M HCl, 1 mM Na-EDTA, 1 mM benzamidine) and flash frozen in liquid nitrogen for storage at -20 °C. Cells were lysed by one freeze-thaw cycle and supplemented with 10 mL of the wash buffer before being homogenized in ice three times (EmulsiFlex-C3). The mixture was centrifuged at 23,000 g for 40 min at 4 °C. The solid pellet was resuspended in 25 ml of the TW buffer (wash buffer with 1% Triton X-100) then centrifuged for 10 min at 12,000 rpm at 4 °C. The wash and centrifuge steps were repeated three times with the TW buffer and once more with wash buffer. The solid pellet was stored at -20 °C. The histones were further purified under denaturing condition with size exclusion and ion-exchange chromatography as described in the following sections.

2.2.2 Histone refolding and purification

Histones H2A, H2B, H3, and H4 were folded into H2A-H2B dimer and (H3-H4)₂ tetramer, then folded into the octamer containing two H2A-H2B dimers and one (H3-H4)₂ tetramer. H2A and H2B or H3 and H4 were first dissolved in the unfolding buffer (7 M guanidinium hydrochloride, 0.02 M Tris-HCl pH 7.5, 0.01M Dithiothreitol) at 2 mg/ml for 1h. The equimolar amounts of histone proteins (either H2A and H2B for H2A-H2B folding or H3 and H4 for (H3-H4)₂ folding) were mixed and dialyzed three times against a fresh 2 L refolding buffer (2M NaCl, 10 mM Tris-HCl pH 7.5, 5 mM 2-mercaptoethanol, 1mM Na-EDTA) at 4°C in a dialysis membrane with a 3500 Da Mw cutoff for 2h, 4h, and overnight. After dialysis, precipitated proteins were removed by centrifugation at 23,000 g for 10 min. Folded histone dimer and tetramer were further purified through a size exclusion column (HiPrep 26/60 sephacryl S-200 HR, Ge Healthcare Life science, Marlborough, MA) at 4 °C.

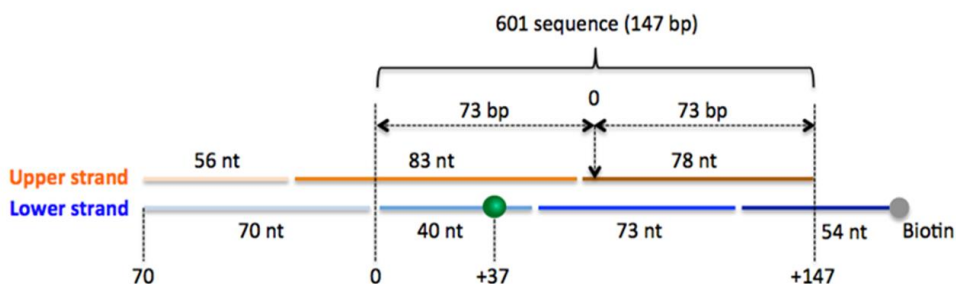
2.2.3 Dye labeling on DNA

A DNA oligo containing an amine group (labeled either along the phosphate backbone or at the side chain inserted to a Thymine base at the C5 position through a 6-carbon linker) was purchased from IDT (Integrated DNA Technologies). The DNA oligo was dissolved in 100ul of the labeling buffer (0.1M NaHCO₃, pH 8.3) to make the final concentration of 30 nmol. The oligo was mixed with 300 nmol Cy3B-NHS ester in DMSO. After 2 hours of incubation at room temperature in the dark, 200 ul phenol-chloroform was added to the mixture. The bottom layer from the mixture was discarded. The phenol-chloroform extraction was repeated until the bottom layer becomes colorless. The mixture was further extracted three times with chloroform. The mixture was added with 3M sodium acetate (pH 5.2) to make a final concentration of 0.3 M sodium acetate. The mixture was added with 3x chilled ethanol and incubated at -80 °C. The mixture was centrifuged at 23,000g for 10 minutes at 4°C. The DNA pellet was rinse with chilled 70% ethanol. The remaining

solvent was removed with a SpeedVac Concentrator (SAVANT DNA120, Thermo scientific).

Figure 1. Nucleosomal DNA construction

Seven DNA fragments with hybridizing overlaps with $T_m > 60^\circ\text{C}$ were annealed and ligated with T4 DNA ligase. The fragments are color-marked in the sequence. The construct is the nucleosomal DNA template containing a Widom 147 bp nucleosome positioning sequence flanked by a 70 bp extranucleosomal DNA linker on one side and 20 nt single-stranded overhangs on the other side terminated by a 5'-Biotin. A Cy3 molecule (FRET donor) is labeled at the nt +37 in the lower strand via conjugation between a C₆-amine group introduced at the Thymine base (UniLinkTM, IDT) and NHS-ester functionalized Cy3.



Upper strand:

5'-AAT GAC CAA GGA AAG CAT GAT TCT TCA CAC CGA GTT CAT CCC TTA TGT GAT GGA CC CTA
TAC GCG GCC GCA TCG GAT GTA TAT ATC TGA CAC GTG CCT GGA GAC TAG GGA GTA ATC CCC
TTG GCG GTT AAA ACG CGG GG G ACAGCGCGTA CGTGCGTTTA AGCGGTGCTA GAGCTGTCTA
CGACCAATTG AGCGGCCTCG GCACCGGGAT TCTCGAT

Lower strand:

5'-/Biotin/GCA TGT AAG TGC ATG TAA GTA TCG AGA ATC CCG GTG CCG AGG CCG CTC AAT TGG
TCG TAG ACA GCT CTA GCA CCG CTT AAA CGC ACG TAC GCG CTG TCC CCC GCG TTT TAA CCG
CCA AGG GGA TTA C TCC CTA GTC TCC AGG CAC GTG TCA GAT ATA TAC ATC CGA T GCG GCC GCG
TAT AGG GTC CAT CAC ATA AGG GAT GAA CTC GGT GTG AAG AAT CAT GCT TTC CTT GGT CAT T

2.2.4 Dye labeling of histone protein

A histone mutant H2BT112C with only one cysteine residue was labeled with maleimide functionalized Atto647N (Sigma Aldrich). The protein was dissolved in the labeling buffer (pH 7.0). Then, 20x molar excess of the dye was added to the histone solution; the dye was dissolved in DMSO before addition. The mixture was incubated for 2 hours at room

temperature and subsequently overnight at 4 °C. Extra dye was removed by buffer exchange with the labeling buffer (pH 7.4) with Zeba spinning desalting columns (Thermo #89891).

2.2.5 Nucleosomal DNA construction

The Widom 601 nucleosomal DNA sequence was used for my experiments (Fig. 1). The entire DNA sequence was divided into several oligonucleotides that were purchased from IDT. The oligonucleotides were dissolved in a TE buffer (10 mM Tris-HCl (pH 8.0), 1 mM EDTA) to make a 20 uL reaction volume containing the oligonucleotides at 5 uM each. The mixture was annealed by heating to 95°C and gradually cooling down to 4 °C in 5 °C steps over 45 minutes in a thermal cycler. The annealed DNA was ligated by 400 units of a T4 ligase (New England Biolabs) in 16 °C for 12 hours. The final DNA solution was purified with a QIAquick PCR purification kit (ID 28106).

2.2.6 Nucleosome reconstitution

The nucleosome core particles were reconstituted by step-wise salt dialysis. The nucleosomal DNA, H2A-H2B dimer, and (H3-H4)₂ tetramer were mixed at 1: ~2.42: ~1.1 (DNA: H2A-H2B: (H3-H4)₂) ratios in the 3xTE buffer with 2 M NaCl on ice for 30 minutes. The mixture was dialyzed via Slide-A-Lyzer MINI Dialysis Tube (10K MWCO, ID 69672, Thermo Fisher Scientific, Waltham, MA) for 1 h in 5 steps of decreasing salt concentrations against TE buffer: 0.85 M, 0.65 M, 0.5 M, 0.3 M, and 0.01 M NaCl.

2.2.7 SDS gel electrophoresis

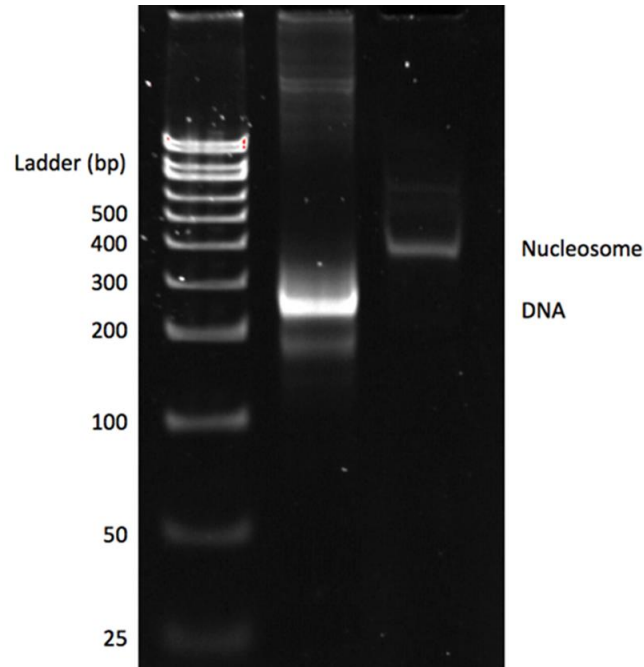
The SDS-PAGE gel was cast by pouring a stacking gel over final resolving gel. The final resolving gel was made with 0.63 mL of 1 M Tris pH 6.8, 0.05 mL of 20 % SDS, 0.83 mL of 40 % acrylamide, 3.4 mL of water, 50 uL of 10 % ammonium persulfate, and 5 uL TEMED. After the final resolving mixture becomes a gel, the stacking gel was poured over the final resolving gel. The stacking gel was made with 3.75 mL of 1 M Tris pH 8.8, 0.05 mL of 20 % SDS, 3.75 mL of 40 % acrylamide, 1.25 mL of water, 100 uL of 10 % ammonium persulfate, and 10 uL TEMED.

2.2.8 Native gel electrophoresis

A 5% native gel was used to check the qualities of DNA and nucleosomes. The native gel was pre-run for 30 minutes at 150 V in a 0.5x TBE buffer at 4 °C. After pre-run, a fresh 0.5x TBE buffer with 50 % sucrose was added to the sample and loaded to the wells. The gel was run for 45 minutes at 150V at 4 °C. The gel was stained by SYBR safe (ThermoFisher Invitrogen) for analysis (Fig. 2).

Figure 2. Native gel showing nucleosome reconstitution

From left to right, they are DNA ladder, DNA, Nucleosome.



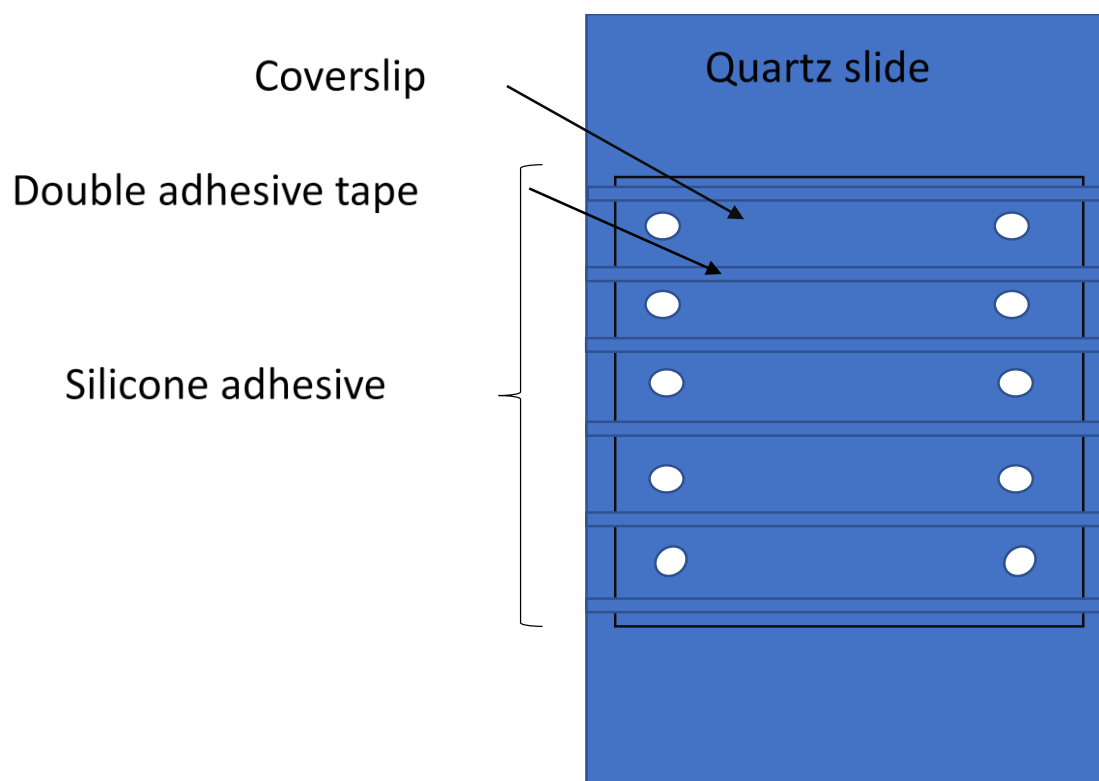
2.3 Single-molecule FRET measurements

2.3.1 Surface functionalization

Quartz microscope slides (G. Finkenbeiner) were drilled with a diamond drill bit (1 mm diameter) for each to have ten holes. (Fig. 3) The slides were soaked in soapy water for 5 minutes. After rinsed with water for 7 times, the slides were immersed in acetone and sonicated for 15 minutes. The slides were subsequently sonicated with dichloromethane for 15 minutes and methanol for another 15 minutes to further remove organic contaminants. The slides were washed with water for 7 times and blow-dried with 99.99 % pure N₂ gas. The slides were further cleaned with a propane-flame for a few seconds to oxidize larger particulate contaminants. After the slides cooled down to room temperature, they were soaked in 1 M potassium hydroxide and sonicated for 15 minutes. After rinsed with water for 7 times, the slides were soaked again in 1 M potassium hydroxide and sonicated for 15 minutes. After rinsed with water for 7 times, the slides were blow-dried with 99.99 % pure N₂ gas. The slides were soaked in a Norchromix® (Sigma) mixture with sulfuric acid overnight. The slides were rinsed thoroughly with water for 7 times and blow-dried with 99.99 % pure N₂ gas.

Figure 3. Cartoon schematic of preparation of the sample chambers.

The white circle represents the holes drilled onto a quartz slide. Five channels were separated by the double adhesive tapes and covered with a coverslip. The left and right edges of the quartz slides were sealed with silicone adhesive.



An aliquot of 8 mg of Biotin-PEG-Silane (3400 MW) was mixed with 10 mg PEG-Silane (2000 MW) in a dried vial. The mixture was dissolved in 50 mL acetonitrile then quickly transferred to the staining jar containing clean microscope slides. The slides were immersed in the solution and sonicated for 15 minutes. The staining jar was emptied and supplied with water followed by sonication for 5 minutes. This rinsing step was repeated once more. The slides were blow-dried with 99.99 % pure N₂ gas and stored under vacuum.

Microscope coverslips were cleaned by flaming with a propane torch and stored under vacuum.

2.3.2 Preparation of sample chamber

A double-sided adhesive tape was cut and placed between holes on the functionalized quartz slides as boundary lines for each channel. The channels were covered with a clean coverslip. The left and right edges of a slide were sealed with epoxy, leaving only two holes open. The slides were illuminated with a UV light for at least 30 minutes to bleach fluorescent contaminants.

Chapter 3. Mechanism of dimer exchange reaction by INO80

3.1 Introduction

Many parts of this chapter are copied from a draft of a manuscript that will be submitted for publication.

Nucleosomes are the fundamental packing unit of DNA in eukaryotes. A nucleosome core particle is made of ~147 base pair (bp) double-stranded (ds) DNA that wraps 1.67 left-handed super-helical turns around a histone protein octamer comprising two copies of H2A, H2B, H3 and H4.¹⁵ The histone core can be broken down to two H2A-H2B heterodimers and one (H3-H4)₂ tetramer at a physiological salt concentration.¹⁶ The structure and structural dynamics of the nucleosome are implicated in gene regulation mechanisms. There are several histone variants that play essential roles in gene regulation.¹⁷ For instance, an H2A variant H2A.Z is enriched in the +1 and -1 nucleosomes immediately flanking a nucleosome depleted region (NDR) of a gene promoter, and has been implicated in both transcription activation and repression.^{18,19,20,21,22,23,24} The structure of a nucleosome core particle containing H2A.Z is nearly identical to that of a canonical particle while its structural dynamics becomes somewhat inhibited although the difference is only marginal.^{25,26} It has been hypothesized that nucleosomes containing H2A.Z-H2B dimers may act as physical barriers to the gene body. A chromatin remodeler SWR1 replaces H2A-H2B with H2A.Z-H2B in these barrier nucleosomes potentially to help keep the genome integrity.^{22,27,28} Another chromatin remodeler in the same family, INO80, replaces H2A.Z-H2B with H2A-H2B, which has been coupled to transcription activation.^{29,5}

INO80, composed of more than 10 subunits, is implicated in diverse genome transactions such as transcription activation, DNA repair, and replication.^{30,31,32} Despite its strong implications in these crucial regulatory and maintenance functions, its mechanisms remain poorly understood. We have previously shown that the dimer exchange function of INO80 is coupled to its translocation activity, based on which we promote a mechanism where unwrapping of DNA upon INO80 translocation destabilizes H2A.Z-H2B in the nucleosome.⁵ This mechanism has also been supported by recent structural analyses of INO80-nucleosome complexes.^{33,34}

The SWR1 and INO80 complexes are members of the INO80 ATP-dependent chromatin remodeler family.^{27,31,32,4} The INO80 family remodelers contain a unique split-ATPase with a long insertion (also called the spacer) present in the middle of the ATPase domain, which distinguishes them from Snf2-like helicases.³⁵ The helicase-related (AAA-ATPase) Rvb1/2 proteins and an Arp (actin-related protein) protein preferentially bind to the spacer domain.^{33,34,35} SWR1 restructures the nucleosome by evicting an H2A-H2B dimer and replacing it with an H2A.Z-H2B dimer.^{27,28} Investigations on the mechanism have resulted in various aspects of the dimer specificity of this reaction. Importantly, the Swc2 subunit of SWR1 is a binding module for H2A.Z-H2B.³⁶ It has also been reported that the Swr1-Z domain recognizes H2A.Z-H2B via its interaction with the alpha-C helix of H2A.Z.⁶ Binding of H2A.Z-H2B to Swc2 and Swr1 is mediated by H2A.Z-specific chaperone Chz1.^{37,38}

Despite the similarities in the subunits between INO80 and SWR1, SWR1 does not slide or evict nucleosomes while INO80 does, suggesting that their mechanisms of dimer exchange may

be unrelated to each other. Their modes of binding to the nucleosome are also different from each other. While both SWR1 and INO80 grasp the nucleosome by binding at two almost opposite sides of the nucleosome, their motor binding site differ from each other as SWR1 motor domain Swr1 binds at the superhelical location (SHL) (+2) and INO80 motor domain Ino80 binds at SHL (-6).^{33,34,35,39} On the other hand, a structural and biochemical basis of dimer specificity of SWR1 may hint on that of INO80. The Ies6 subunit of INO80 is a homolog of the Swc2 subunit of SWR1 and has been suggested to recruit Arp5.^{36,40,8} It has been shown that Arp5 in the Arp5/Ies6 module interacts with the acidic patch on H2A-H2B in nucleosomes and also with free H2A-H2B in solution.^{33,41} It would, therefore, be reasonable to postulate that Arp5/Ies6 would interact more strongly with H2A.Z-H2B with their enhanced acidic patch. As the Swc2 subunit makes SWR1 bind stronger to H2A.Z-H2B than H2A-H2B, Arp5/Ies6 may also drive preferential binding of INO80 to H2A.Z-H2B over H2A-H2B. Other than this hint, nearly nothing is known about the dimer specificity of the INO80-induced dimer exchange reaction.

Here we investigated the mechanism of the dimer exchange reaction by INO80 based on three-color single-molecule FRET measurements.^{5,42,43} We observed that INO80 unwraps DNA while it progresses through the nucleosome, and translocates back and forth multiple times near the proximal dimer-DNA interface. Results indicate that the back-and-forth motion of INO80 coincides with attempts of dimer exchange. We found that out of all 4 possibilities of dimer exchange specificity (i.e., H2A.Z-H2B \rightarrow H2A.Z-H2B, H2A.Z-H2B \rightarrow H2A-H2B, H2A-H2B \rightarrow H2A.Z-H2B, H2A-H2B \rightarrow H2A-H2B), only the H2A.Z-H2B \rightarrow H2A-H2B case results in significant activity. Based on these results, we suggest that the specificity of dimer exchange by INO80 may stem from its potentially stronger binding to H2A.Z-H2B than to H2A-H2B, a mechanism unrelated to that of SWR1, which has also been hypothesized to be due to its preferential binding to H2A.Z-H2B.

3.2 Materials and Methods

Histone purification, nucleosomal DNA preparation, and nucleosome reconstitution protocols are described in chapter 2. The INO80 complex was obtained from a collaborator.

Histone H2A.Z-H2B dimer exchange kinetics measurement with three-color smFRET

For the three-color smFRET measurements to investigate the kinetics of dimer exchange, we used our previously published setup and method.^{42,43} The nucleosomes containing Atto647N labeled H2A.Z-H2B (or H2A-H2B) in a buffer containing 10 mM Tris-HCl at pH 8.0, 1 mM EDTA and 10 mM NaCl was injected into a sample chamber constructed on a polyethyleneglycol (PEG) coated microscope slide that was pre-incubated with streptavidin followed by a thorough wash. The nucleosomes were incubated for 7 minutes followed by a thorough wash with a buffer (10 mM Tris-HCl at pH 8.0, 0.05% tween 20). A reaction mix was prepared by adding 2 nM INO80 and 5 nM Cy5.5-H2A-H2B (or Cy5.5-H2A.Z-H2B) to a buffer (20 mM Tris-HCl, pH 8.0) containing 5 mM MgCl₂, 1 mM ATP, 5 % glycerol, 20 mM KCl, 50 mM NaCl, 0.05 % Tween 20, 1 mM DTT, 0.1 mg/ml BSA, 0.4 U/mL protocatechuate-3,4-dioxygenase (PCD), 4 mM protocatechuic acid (PCA), and 1 mM Trolox. The reaction mix was injected into the sample

chamber, which was immediately followed by three-color smFRET imaging with 350 ms frame integration consecutively for 5 minutes. As the labeling efficiency of the histone dimer in the nucleosome is at 50 %, we must have a 25 % chance detecting a nucleosome that shows the FRET efficiencies as designed. Counting only the nucleosomes showing FRET, we will have a ~33 % of chance detecting a properly labeled nucleosome. The other 67 % of the nucleosomes (i.e. both dimers labeled or the distal dimer labeled) were excluded from further analyses based on their relative initial fluorescence levels (i.e. near 100 % FRET from Cy3 to Atto647N indicates both dimers labeled and too low Atto647N fluorescence level compared to Cy3 indicates distal dimer labeled).

Histone H2A.Z-H2B dimer exchange efficiency measurements with three-color smFRET

For the three-color smFRET assay to measure the efficiency of dimer exchange, we used our previously published setup and method.⁴³ For this assay, 1 nM of the nucleosomes containing Atto647N labeled H2A.Z-H2B (or H2A-H2B) were incubated with 2 nM INO80 and 5 nM Cy5.5-H2A-H2B (or Cy5.5-H2A.Z-H2B) in a buffer (20 mM Tris-HCl, pH 8.0) containing 5 mM MgCl₂, 1 mM ATP, 5 % glycerol, 20 mM KCl, 50 mM NaCl, 0.05 % Tween 20, 1 mM DTT, 0.1 mg/ml BSA, and 1 mM Trolox. After 30 min incubation on ice, the mixture was diluted 5-fold with the same buffer followed by an injection to a sample chamber on a microscope slide that was pre-incubated with 0.5 μM streptavidin for 15 minutes followed by a thorough wash. The fluorescence signals from the three fluorophores were collected through a water-immersion objective lens. Images were taken with iXon Du-897 camera (Andor Technology, Belfast, Ireland) consecutively with 350 ms integration for 2 minutes. Imaging was repeated for 50 times per case. As the labeling efficiency of the histone dimer in the nucleosome is at 50 %, we had a ~33 % of chance detecting a nucleosome that shows the FRET efficiencies as designed, as was described above. The other 67 % of the nucleosomes (i.e. both dimers labeled or the distal dimer labeled) were excluded from further analyses based on their relative initial fluorescence levels (i.e. near 100 % FRET from Cy3 to Atto647N indicates both dimers labeled and too low Atto647N fluorescence level compared to Cy3 indicates distal dimer labeled).

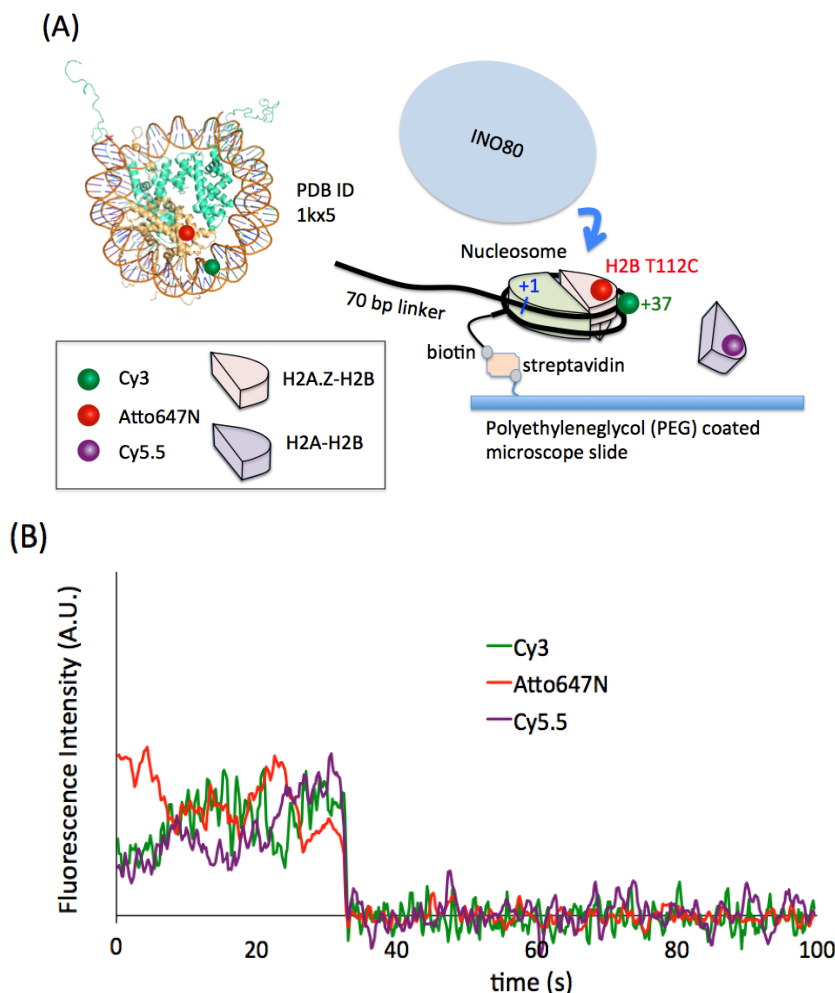
3.3 Results

Nucleosomal DNA unwraps as INO80 translocates

The experimental setup to monitor the real-time dimer exchange reaction is shown in figure 4. For the three-color smFRET instrumental setup, we used our previously published one.^{42,43} The nucleosome with a 70 bp linker is immobilized on a polyethyleneglycol (PEG) coated microscope quartz slide via streptavidin-biotin conjugation (Fig. 1). Another 20-nucleotide single-stranded DNA linker was added to the biotinylated distal end of the nucleosome in order to avoid any unwanted contact between the nucleosome and the surface. The nucleosome is labeled at the +37th nucleotide from the entry (+1) site of the nucleosome (Fig. 4A) via NHS-ester functionalized Cy3 conjugation to an amine group linked to the Thymine base (Amino Modifier C6 dT from IDT) and

at the H2A.Z T112C with maleimide functionalized Atto647N. This FRET pair location will report disruption of the strong H2A.Z-H2B/DNA to interface near the superhelical location SHL (-3) and SHL (-4) and

Figure 4. Experimental setup to investigate the histone H2A.Z-H2B dimer exchange reaction by INO80. A nucleosome core particle with a 70 bp linker to the entry side for INO80 activity and a 20 nt linker for surface immobilization is conjugated to the surface via biotin-streptavidin interaction. The FRET donor (Cy3) is labeled at the +37th nucleotide, which will report disruption of the strong H2A.Z-H2B/DNA interface near the SHL (-3) and SHL (-4). Purified INO80 complexes and free histone H2A-H2B dimers are injected and subsequent fluorescence changes from the three fluorophores (Cy3, Atto647N, and Cy5.5) that form a three-color FRET system. (B) A representative set of fluorescence time trajectories of the three fluorophores recorded upon injection of INO80 to the reaction chamber. Background fluorescence levels have been subtracted, but no inter-channel leakage has been corrected.



SHL (-4). Intact nucleosomes that are properly labeled (Fig. 4) show a high level of Atto647N fluorescence and a low level of Cy3 due to FRET. We had approximately a one-third chance to

find these nucleosomes among all nucleosomes showing FRET, which is what we expected based on the near 100 % dimer labeling efficiency (see the method section). The other two thirds of the nucleosomes with the distal dimer labeled or both dimers labeled were discarded. As we cannot precisely quantify the three-way FRET efficiencies at various stages of the nucleosomal dynamics during the INO80 reaction, we did not correct the inter-channel leakage between Atto647N and Cy5.5. This approach will enable us to unambiguously analyze the nucleosomal changes at the cost of disabling distance measurements which is not needed for our investigation. The leaked Atto647N fluorescence to the Cy5.5 channel is at an approximately similar level to Cy3 fluorescence as can be seen in the first few seconds of the fluorescence intensity time trajectories in figure 5. Upon injection of INO80 and ATP, complex FRET changes were observed, indicating that multi-step structural changes are taking place in the nucleosome. In the absence of INO80 or ATP, no FRET change was detected at least within the first 10 minutes of observation. This result indicates that INO80 induced the structural changes in the nucleosome during its remodeling activity.

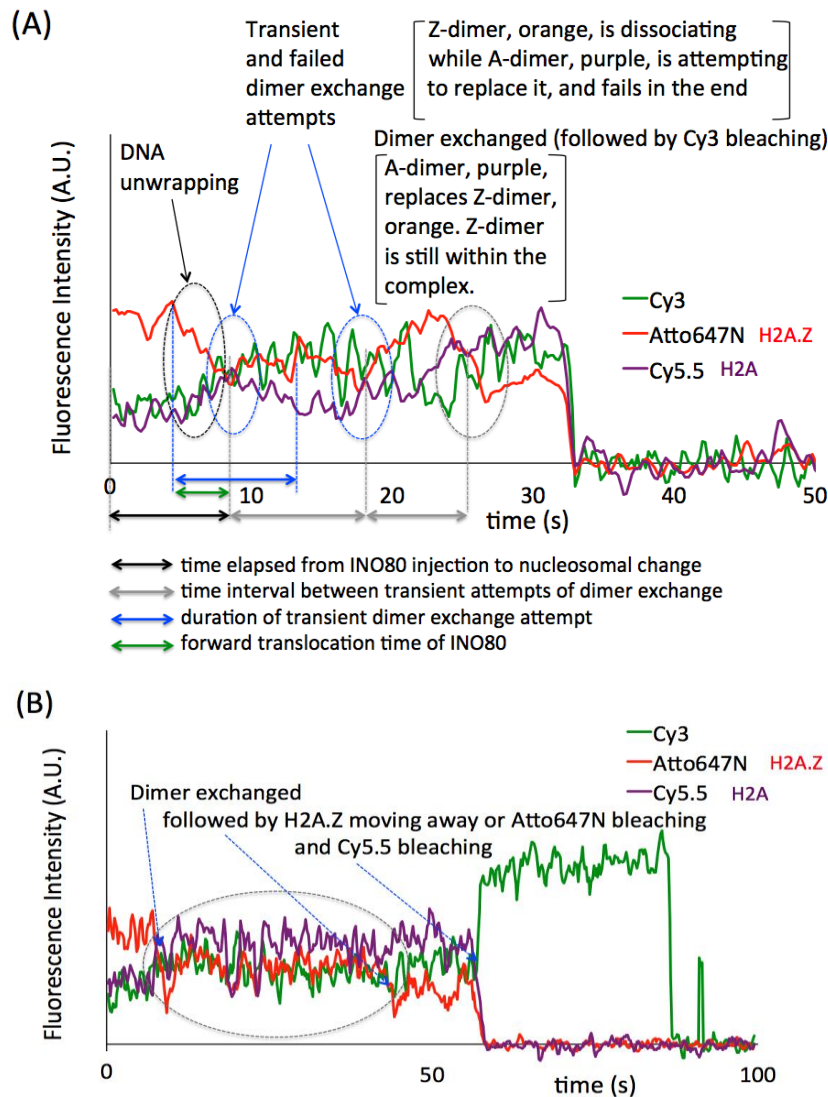
For further investigation of the nucleosomal changes, we collected and analyzed the smFRET data during the first 5 minutes after INO80 injection. We made observations of total 749 intact nucleosomes that are properly labeled with the three fluorophores out of which 91.4 ± 6.2 % (690 nucleosomes, $N = 3$, $n = \{197, 256, 296\}$) show dynamic FRET changes. Two sets of time trajectories of the changes are shown in figure 5. The decreasing FRET acceptor (Atto647N) fluorescence and concomitantly increasing FRET donor (Cy3) fluorescence at around the 10 sec time point in figure 5A indicates either DNA is unwrapping at the H2A.Z-H2B/DNA interface near SHL (-3) and SHL (-4) or that H2A.Z-H2B (Z-dimer) is dissociating, which must be induced by INO80 activity. As INO80 activity is coupled to its translocation along nucleosomal DNA, it must accompany DNA unwrapping, which is also supported by recent structural analyses.^{33,34} Another possibility is to have the DNA kept completely intact while the Z-dimer is displaced upon INO80 translocation through the DNA-dimer contact region although this is extremely unlikely considering that INO80 must have already broken the DNA-dimer interface during its translocation. Therefore, we conclude that the fluorescence changes are due to DNA unwrapping regardless of whether they may also be due to concomitant dimer displacement.

Exchanging H2A-H2B dimer is a part of INO80 complex translocating along DNA

All of the 690 nucleosomes with dynamic FRET changes show a clear sign of Atto647N decrease and Cy3 increase, implying DNA unwrapping upon INO80 injection which may accompany Z-dimer displacement. In addition, 638 or 92.5 % of the 690 nucleosomes always show a concomitant increase in the Cy5.5 fluorescence, indicating that DNA unwrapping and possibly concomitant Z-dimer displacement always accompany H2A-H2B (A-dimer) approaching the DNA-dimer interface. The level of Atto647N fluorescence eventually becomes lower than that of Cy5.5 at the end of figure 5A and in the middle of figure 5B (gray circles), showing that the A-dimer successfully replaces the Z-dimer. These observations strongly suggest that A-dimer insertion,

DNA unwrapping, and Z-dimer dissociation take place simultaneously within our observation time

Figure 5. Real-time smFRET dynamics reveals how histone H2A.Z-H2B (Z-dimer) is exchanged with H2A-H2B (A-dimer) by INO80. (A) Three-color fluorescence intensity time trajectories (see figure 4 for setup) show that (1) DNA unwraps as INO80 binds and translocates along the nucleosome (0 – 5 sec, black circle), (2) Z-dimer exchange takes place after multiple attempts (5 – 30 sec, blue circles), and (3) A-dimer approaches concomitantly with Z-dimer dissociation (blue and gray circles). Within the gray circle, it is evident that there is a two-step change in the fluorescence intensities. The first step is likely due to dimer exchange and the second is likely due to Z-dimer moving away from the site or its fluorophore (Atto647N) photobleaching. See (B) for another clearer example of this two-step change. (B) Another example shows an elongated dimer exchanged state before the Z-dimer moves away or its fluorophore (Atto647N) photobleaches, suggesting that exchanged Z-dimer stays within the nucleosome/INO80 complex before it moves away or photobleaches.



resolution of 350 ms. This result indicates that the INO80 action responsible for DNA unwrapping and Z-dimer displacement must also induce A-dimer insertion. As INO80 translocation along DNA is what induces DNA unwrapping and concomitant or subsequent Z-dimer displacement, we conclude that INO80 translocation is also what catalyzes A-dimer insertion. Two viable scenarios for the mechanism is (i) that the two dimers spontaneously replace each other when the Z-dimer is displaced by INO80, and an exchanging A-dimer is available in solution or (ii) that the A-dimer exchanging the Z-dimer is a part of the INO80 complex translocating along the DNA so that when the Z-dimer is displaced from the nucleosome the A-dimer is readily available for exchange. As we previously reported, INO80 mobilizes Z-dimer containing nucleosomes faster than A-dimer nucleosomes, supporting both of these scenarios. What differentiates these scenarios is during the exchange whether A-dimer insertion takes place spontaneously from the solution or is mediated by INO80. We further investigated these scenarios based on the dimer specificity of the reaction.

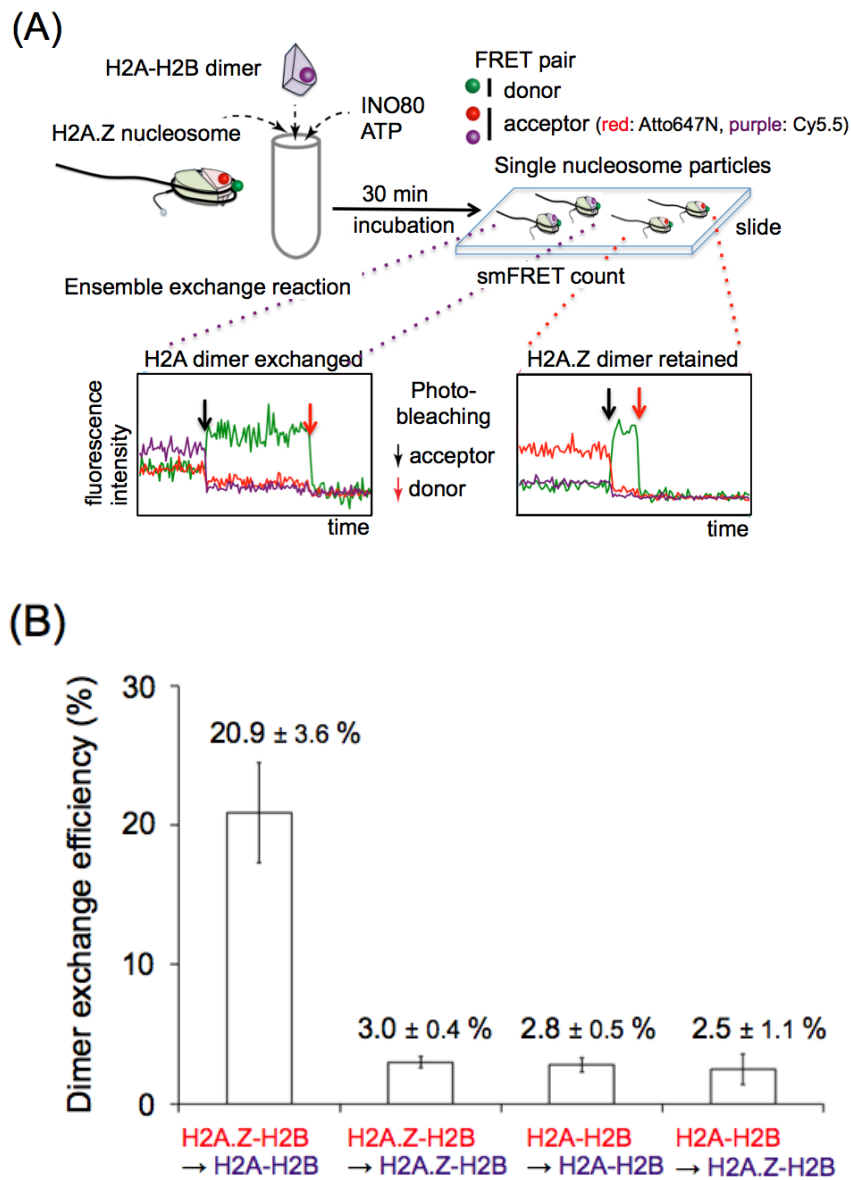
Dimer specificity of exchange may be due to preferential binding of INO80 to H2A.Z-H2B.

We measured the dimer exchange efficiencies in all four combinations of dimers (i.e. A- to Z-, Z- to A-, A- to A-, and Z- to Z-dimer exchange) in order to investigate the dimer specificity of the reaction. To measure the dimer exchange efficiencies, we constructed another experimental setup that we have reported previously.¹⁶ As depicted in figure 6A, we pre-mixed the nucleosome and INO80/ATP in a microtube and incubated for 30 minutes. The nucleosomes were immobilized on a PEG coated microscope slide and inspected visually if they had the dimer retained or exchanged. The measurements were continued for 90 minutes after immobilization. The results are shown in figure 6B, revealing that only the Z- to A-dimer exchange case shows a significant level of activity.

As described above, Z-dimer nucleosomes are mobilized faster than A-dimer nucleosomes, which should play a major role in determining the dimer specificity. However, if the specificity depends solely on this preferential mobilization and the exchanging dimer insertion takes place spontaneously from the solution, Z- to Z-dimer exchange should be as efficient as Z- to A-dimer exchange, which is not the case. Therefore, these results indicate that the dimer specificity should also be implemented during the exchange. This conclusion implies that the identity of the exchanging dimer also matters to the reaction efficiency, leading to a conclusion that the second scenario described above is more viable where the exchanging dimer is a part of the INO80 complex. As for the mechanism of how this scenario results in the dimer specificity, we propose that it is due to the relative stability of the two dimers in the nucleosome and on INO80. Assuming no difference in the nucleosome stability with A- or Z-dimers, the dimer specificity during exchange should be due to preferential binding of INO80 to a Z-dimer over an A-dimer. Under this proposal, when there are two labile dimers competing against each other's binding site (i.e. one in the nucleosome and the other on INO80), their exchange efficiency would be set by their relative binding preferences toward the two sites. INO80 contains Ies6, a homolog of Swc2 that binds more strongly to a Z-dimer than to an A-dimer.^{36,8,44} We suggest that this potential binding preference of INO80 to a Z-dimer is the basis of the dimer specificity during the exchange. This specificity can also explain the preferential mobilization of the Z-dimer containing nucleosome. In the absence of exchanging dimer, Z-dimer should find it more beneficial to transfer from the nucleosome to INO80 than A-dimer would if INO80 binds more strongly to Z-dimer. All of these

results and interpretations support the second scenario that the exchanging A-dimer is a part of the INO80 complex translocating along the DNA.

Figure 6. INO80 exchanges only H2A.Z with H2A out of all four cases of dimer identity combinations. (A) Experimental setup to measure the efficiency of dimer exchange by INO80 at a single-nucleosome level based on three-color FRET. Nucleosomes with a FRET pair with Cy3 (DNA) and Cy5.5 (H2A-H2B dimer or H2A.Z-H2B dimer) or Atto647N (H2A.Z-H2B dimer or H2A-H2B dimer) were identified and counted to give the dimer exchange efficiency. The acceptor is photobleached at a single time point (black arrow), followed by a single-step Cy3 photobleaching (red arrow). (B) The results are shown for the efficiencies of all four cases.



Dimer exchange by INO80 takes place via multiple steps

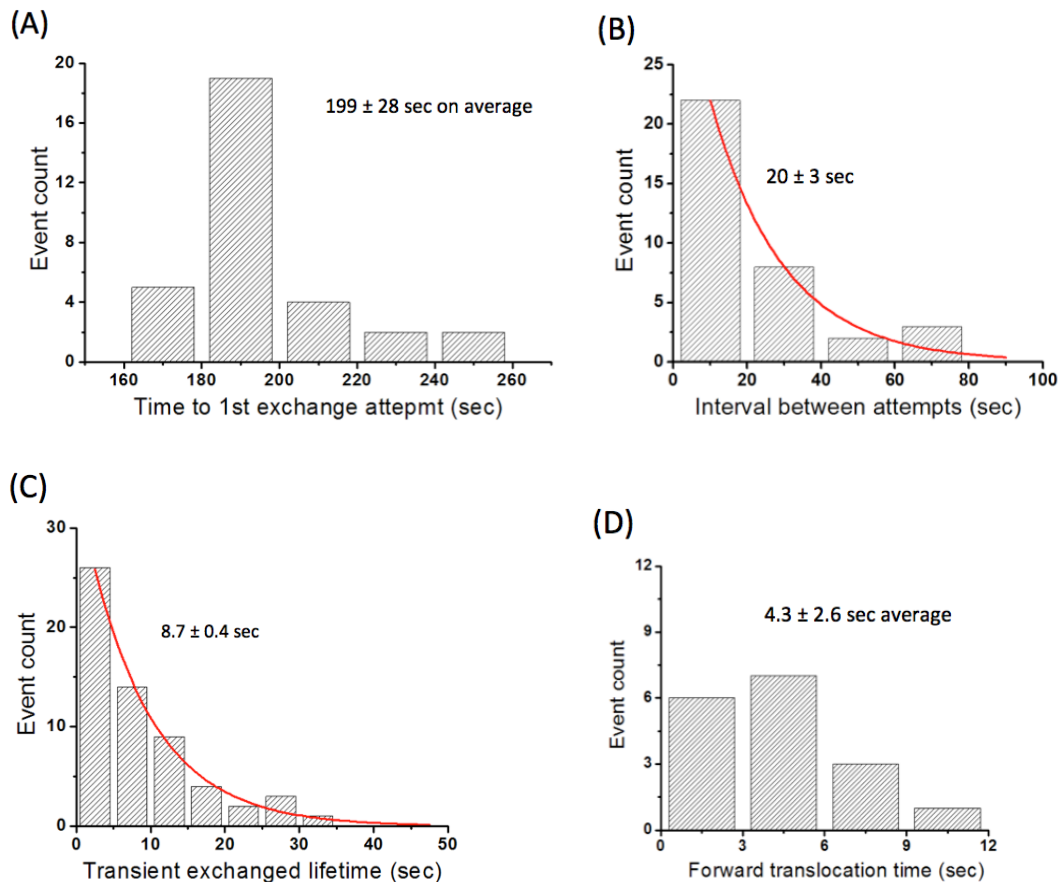
A noteworthy smFRET signature of the dimer exchange reaction is that the A-dimer approaching events (blue circles in figure 5A) are more often transient than persistent (gray circles at the end of figure 5A and in the middle of figure 5B), suggesting that multiple attempts may be necessary before the A-dimer successfully replaces the Z-dimer. The smFRET signal also suggests that the exchanged Z-dimer remains in the nucleosome/INO80 complex. It is evident in figures 5A and 5B that the fluorescence levels upon dimer exchange show two-step changes (gray circles in figures 5A and 5B). The first step is indicative of dimer exchange because the two acceptor fluorescence levels cross each other, resulting in stronger Cy5.5 fluorescence than Atto647N fluorescence. The second-step should be due either to Z-dimer moving away further from the exchanged site or to its fluorophore (Atto647N) photobleaching. In either case, the existence of the second-step indicates that the Z-dimer remains in the INO80/nucleosome complex after exchange.

Our proposed mechanism summarizes that INO80 harbors an A-dimer and it exchanges the A-dimer with the nucleosomal Z-dimer upon translocation along DNA and mobilization of the nucleosome (i.e. DNA unwrapping and dimer displacement). In order to measure the kinetic rate constants of each step, we further analyzed the smFRET time trajectories. For the kinetic rate constant analyses for DNA unwrapping and/or dimer displacement, we filtered the 690 nucleosomes and selected the nucleosomes with long enough photobleaching lifetimes to show >2 regions with a steady Atto647N/Cy3 fluorescence level so that we can clearly analyze the inter-state FRET dynamics without introducing any artifact due to premature fluorophore photobleaching. This selection left 32 nucleosomes. Despite the relatively small size of the sample, the FRET state duration and formation frequency histograms in figure 7B-C verify that the data is of sufficiently high quality to yield rate constants with a small error ($\leq 15\%$ of the average values). We also constructed the histogram of the elapsed time between INO80 injection and the onset of DNA unwrapping (Fig. 7A). The average is 198 ± 28 sec. This time convolves INO80 effective binding to the nucleosome and translocation to an unknown DNA-histone contact point where INO80 starts unwrapping DNA, causing a FRET change. The biphasic shape of the event counts in figure 7A also supports that this time is a convolution of multiple steps as the smFRET time trajectories in figure 5 and the process time histogram in figure 7D indicate that the translocation-induced DNA unwrapping takes only on the order of a few seconds, this time of 198 ± 28 sec must be mostly spent on effective binding of INO80 to the nucleosome. Combining the rate constants converted from these process times, the mechanism of INO80 dimer exchange reaction with rate constants is illustrated in figure 8.

According to the mechanism, INO80 first binds the nucleosome and translocates along the nucleosomal DNA until it stalls at a strong DNA-histone contact region that is likely at the Z-dimer-DNA interface. The kinetic rate constant of binding and translocation up to this point should be the reciprocal of the average time to reach there (Figs. 5A and 7A). This estimation leads to $k = 1/(198 \pm 28 \text{ sec})/nM_{\text{INO80}} = 5.05 \pm 0.71 \times 10^{-3} \text{ sec}^{-1}\text{nM}^{-1}_{\text{INO80}}$. As this number is from per immobilized nucleosome, the rate needs to be corrected accordingly to the masses of the nucleosome and INO80 if one were to obtain a value for a freely diffusing nucleosome particle and INO80.

Upon binding, INO80 translocates along the nucleosomal DNA, resulting in smFRET changes (Fig. 7A). The transient, multiple, and simultaneous Atto647N and Cy5.5 fluorescence

Figure 7. Process times of histone H2A.Z-H2B dimer exchange by INO80 reveal the kinetic rate constants of the reaction steps. (A) A histogram of the elapsed time to observe nucleosomal dynamics from INO80 injection. See the black arrow in figure 5A. This is approximately the inverse of the effective INO80 binding rate to the nucleosome. (B) A histogram of interval between two consecutive dimer exchange events. See the gray arrows in figure 5A. This time constant is the inverse of the rate constant of the transient dimer exchange attempts. (C) A histogram of the duration of the state where H2A.Z-H2B is transiently exchanged by H2A-H2B. This time was measured from the beginning of the FRET change to the end of the FRET change as depicted in figure 5A (blue circles and arrows). The time resolution of the histogram is set to 5 sec in order to make any error in arbitrarily pinpointing the starting and ending FRET times negligible. (D) A histogram of the process time for INO80 forward translocation from the first binding site to the first stalled position. See the green arrow in figure 5A.

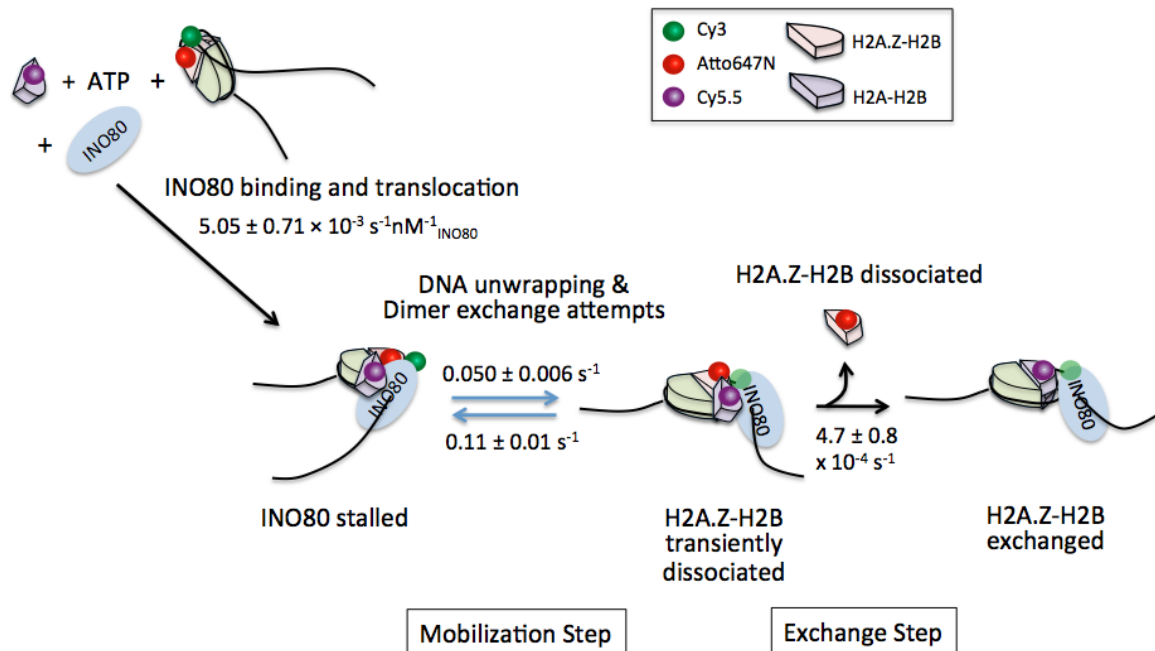


changes should correspond to transient, and multiple A-dimer insertions attempt concomitant to DNA unwrapping and Z-dimer displacement. As was concluded above, we can explain these observations with a mechanism that the A-dimer is a part of the translocating INO80 complex, as

depicted in figure 8. According to the histograms in figure 7, the time intervals between two transient attempts of dimer exchange is on average 20 ± 3 sec (Fig. 7B), and the duration of the transient A-dimer insertion attempts are on average 8.7 ± 0.4 sec (Fig. 7C). The kinetic rate constants should be directly the inverses of these time constants (i.e. $1 / (20 \pm 3 \text{ sec}) = 0.050 \pm 0.006 \text{ sec}^{-1}$ and $1 / (8.7 \pm 0.4 \text{ sec}) = 0.11 \pm 0.01 \text{ sec}^{-1}$).

Lastly, upon multiple failed attempts, the Z-dimer is successfully replaced by the A-dimer. In order to estimate this rate constant, we measured the dimer exchange efficiency after 30 min incubation with INO80/ATP and counting the number of nucleosomes with an A-dimer for the next 1 hour. The sign is stable A-dimer fluorescence (i.e. Cy5.5 fluorescence, purple line in figure

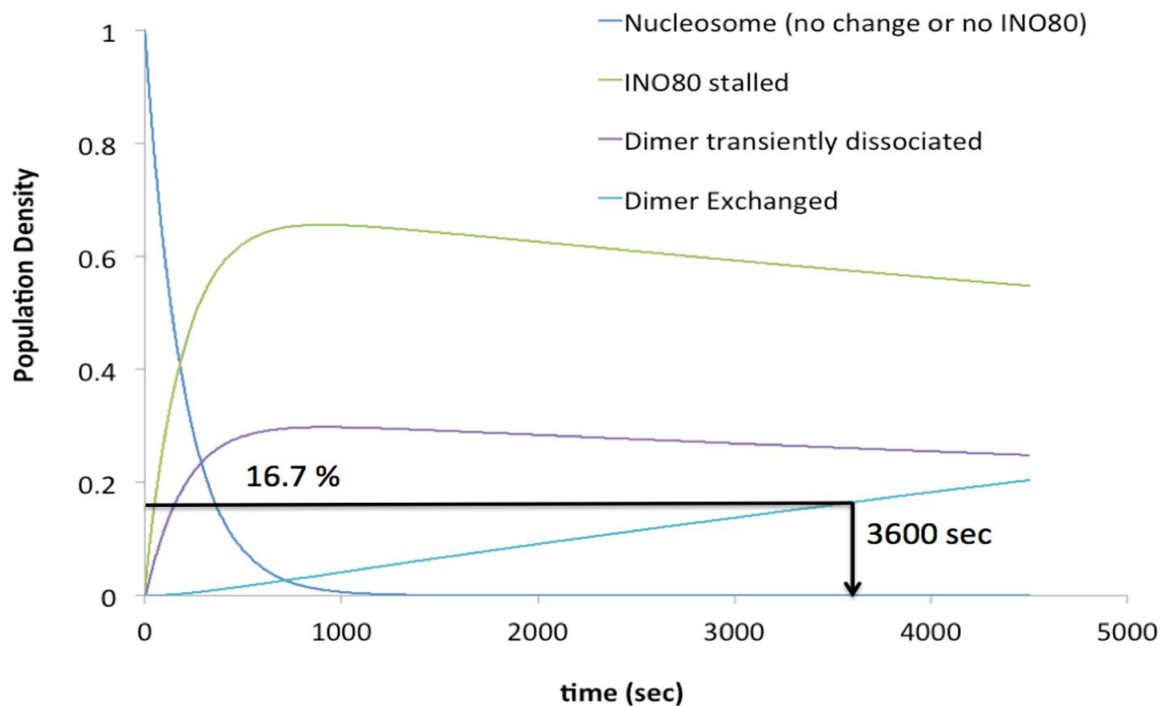
Figure 8. Suggested mechanism of H2A.Z-H2B dimer exchange by INO80. INO80 first binds the nucleosome properly for remodeling. INO80 translocates along the nucleosome and unwraps DNA, inducing partial and transient dissociation of H2A.Z-H2B. INO80 eventually stalls at the H2A.Z-H2B/DNA interface and back-slips due to the built-up mechanical force. During this course of events, H2A-H2B dimer approaches the H2A.Z-H2B site as H2A.Z-H2B transiently dissociates, suggesting that H2A-H2B is a part of the translocating INO80 complex. Upon repeated such attempts, H2A.Z-H2B is finally replaced by H2A-H2B.



5B) higher than the Z-dimer fluorescence (i.e. Atto647N fluorescence, the red line in figure 5B) as we also reported previously.⁵ We observed a total 1036 nucleosomes and 173 of them showed the dimer exchanged ($= 16.7 \pm 1.2 \%$, error obtained from the standard deviation of a binomial distribution with $p = 0.167$). We simulated the reaction scheme shown in figure 8 with all the rate constants to match the final dimer exchange rate of 16.7 % at the 60 min time point (Fig. 9). We approximated the reaction time to be 60 min that is the halfway between the 30 min incubation

time and 1 hour measurement time. This simulation results in the final step rate constant of $1.7 \pm 0.3 \times 10^{-4} \text{ sec}^{-1}$. Our measurements also revealed a small number of nucleosomes (17 nucleosomes out of 1036 observed = 1.6 %) showing loss of the Z-dimer without A-dimer insertion. This small

Figure 9. Statistics of the dimer exchange efficiencies and Population changes of the various intermediates during dimer exchange by INO80



	Z to A	Z to Z	A to A	A to Z
Exchange efficiency	20.9%	3.0%	2.8%	2.5%
Standard deviation	3.6%	0.4%	0.5%	1.1%
Sample size	139	135	89	165
	115	154	130	144
	144	119	113	115
Total sample size	398	408	332	424

population also supports our mechanism that INO80 translocation induces high flexibility of the Z-dimer and prepares it for exchange with another dimer available nearby. As INO80 translocates with an A-dimer according to our mechanism, the Z-dimer is replaced by an A-dimer transferred from INO80.

3.4 Discussion

Based on single-molecule observations of individual nucleosomes in a three-color smFRET setup, we propose a mechanism of histone H2A.Z-H2B dimer exchange by INO80. The three key aspects of the mechanism are that INO80 translocation through the DNA-dimer contact region requires multiple attempts, that the exchanging H2A-H2B dimer is a part of the INO80 complex translocating along DNA, and that the dimer specificity is rendered by the preferential binding of INO80 to H2A.Z-H2B over H2A-H2B.

We have previously reported that INO80 dimer exchange activity is coupled to its translocation by showing that the nucleosome with nicked or gapped DNA does not show any dimer exchange activity.⁵ In the present report, we suggest that dimer exchange is driven by destabilization of H2A.Z-H2B upon INO80 translocation near the DNA-dimer contact region. This notion is also supported by the recent cryo-EM structures of INO80-nucleosome complexes.^{33,34} In the structures and their analyses, the motor domain (Ino80) binds the nucleosomal DNA at the SHL (-6). In both human and fungal INO80 complexes, the Arp5-Ies6 module also anchors to the nucleosome on the opposite side near the DNA/H2A.Z-H2B region at the SHL (-2) and SHL (-3). This double-anchoring will make INO80 translocation generate mechanical force applied to the DNA, which should induce DNA unwrapping from the histone core or separation of DNA-H2A.Z-H2B altogether from the nucleosome core. Therefore, upon the Ino80 motor action, the interface between DNA and H2A.Z-H2B or that between DNA-H2A.Z-H2B and INO80 would need to be broken at least partially to accommodate the mechanical force. We have previously reported that under a high-salt condition (650 mM NaCl) or in the presence of histone chaperone, DNA-H2A.Z-H2B separation altogether from the nucleosome core is negligible compared to DNA unwrapping from the histone core.⁴³ As this type of mechanical force has also been previously reported to induce DNA unwrapping from the histone core, we conclude that the Ino80 motor action would induce DNA unwrapping from the H2A-H2B surface^{45,46,47}, which is in good agreement with our smFRET observation. Upon DNA unwrapping around this region, H2A.Z-H2B would become unstable and labile for exchange. The basal levels of non-specific dimer exchange (Fig. 6) and a small population of nucleosomes showing dimer eviction without exchange also support this conclusion.

Based on our smFRET observation, we can estimate how fast INO80 translocates along nucleosomal DNA from the binding site to the DNA/H2A.Z-H2B interface. The forward translocation time of INO80 (4.3 ± 2.6 sec, Fig. 7D) likely corresponds to translocation to the DNA-dimer contact region near SHL (-3) and (-4). Taking the average distance to these two SHLs, we estimate that this site is at the 25th nucleotide from the Ino80 binding site at the SHL (-6), resulting in the translocation rate of 170 ± 100 ms/nt. This is a much slower rate than a typical RNAPII elongation rate at a few tens of milliseconds per nucleotide. We suggest that this slow

rate is likely due to double-anchoring of INO80 to the nucleosome, resulting in a mechanical force upon INO80 translocation.

The dimer exchange reaction according to this conclusion is a spontaneous process when a nucleosomal dimer becomes sufficiently unstable, and a free dimer for exchange is available nearby. Based on the dimer specificity measurements (Fig. 6), we propose that the exchanging dimer is provided by INO80. As a separate Arp5-Ies6 module can bind an H2A-H2B dimer and a nucleosome particle free in solution, we suggest that it may act as the binding site for an H2A-H2B dimer that will eventually replace a nucleosomal dimer. The smFRET time trajectories clearly show that Z-dimer displacement or DNA unwrapping always takes place concomitantly with A-dimer insertion or approach, which is strong support to our hypothesis. If dimers free in the solution can exchange the nucleosomal dimer that became labile due to INO80 penetration, we would have observed nearly identical rate for Z- to Z-dimer exchange to that for Z- to A-dimer exchange, which was not the case (3.0 ± 0.4 % vs. 20.9 ± 3.6 %). These observations suggest that the nucleosome-INO80/H2A-H2B complex forms a tight structure around the H2A.Z-H2B whose site is not easily accessible from the solution even when H2A.Z-H2B became labile.

We observe multiple dimer exchange attempts that eventually lead to a successful exchange. According to the previous biochemical results and structural analyses, INO80 may keep pumping DNA into the nucleosome until a high enough tension or torque can build up that can persistently destroy the nucleosome structure at the Arp5-Ies6/DNA/H2A.Z-H2B interfaces.^{33,34} Our observation suggests that this can happen only after multiple failed attempts. After a failed attempt, INO80 can slip back to the starting point, which would release the mechanical force built up during multiple ATP hydrolysis cycles. What may facilitate successful forward progression through this region is the simultaneous dimer insertion and dissociation. In the absence of the exchanging dimers, these multiple attempts may eventually lead to nucleosome mobilization.

From a thermodynamics perspective, in order for such a spontaneous dimer exchange for taking place, the dimer stabilities need to improve upon the transaction. In other words, the dimer exchange efficiency should be determined by the strength of INO80 interaction with the nucleosomal dimer to that with the exchanging dimer. According to our results in figure 6, INO80 should interact more strongly with H2A.Z-H2B than with H2A-H2B. No results are available on the relative interaction strengths of INO80 with these two dimer species. We suggest that the component responsible for this preferential binding may be Ies6, a homolog of Swc2 in SWR1 rendering stronger H2A.Z-H2B binding over H2A-H2B, in combination with Arp5 that can bind H2A-H2B free in solution.³³ It has also been shown that Arp5 in the Arp5/Ies6 module interacts with the acidic patch on H2A-H2B in nucleosomes.⁴¹ Therefore, it is reasonable to postulate that Arp5/Ies6 interact more strongly with H2A.Z-H2B than with H2A-H2B due to the enhanced acidic patch of H2A.Z-H2B.

Despite the similarities between INO80 and SWR1, they may work in unrelated mechanisms during dimer exchange, which is supported by their functional and structural differences. SWR1 does not slide or evict nucleosomes while INO80 does. Their modes of binding to the nucleosome are also different from each other. While both SWR1 and INO80 anchors at two sites on the nucleosome at SHL (+2) and SHL (+6) for SWR1 and at SHL (-2)/(-3) and SHL (-6)

for INO80, their motor domains bind at the opposite side to each other as Swr1 binds at SHL (+2), and Ino80 binds at SHL (-6).^{33,34,35} Therefore, remodeling by Swr1 would be likely to the opposite direction to that by Ino80 . These results suggest that SWR1 likely acts via a mechanism unrelated to that of INO80.³⁵

References

1. CM. Weber, S. Ramachandran, S. Henikoff, Nucleosomes Are Context-Specific, H2A.Z-Modulated Barriers to RNA Polymerase. *Cell* **290**, 1–11 (2015).
2. Karine Jacquet and Jacques Côté, DNA repair: Chromatin remodeling without H2A.Z? *Cell Cycle* **13**, 1059 (2014).
3. CB. Gerhold, & SM. Gasser, INO80 and SWR complexes: Relating structure to function in chromatin remodeling. *Trends Cell Biol.* **24**, 619–631 (2014).
4. C. R. Clapier, & B. R. Cairns, The Biology of Chromatin Remodeling Complexes. *Annu. Rev. Biochem.* **78**, 273–304 (2009).
5. Sandipan Brahma, Maheshi I. Udugama, Jongseong Kim, Arjan Hada, Saurabh K. Bhardwaj & Solomon G. Hailu, T.-H. Lee & B. Bartholomew, INO80 exchanges H2A.Z for H2A by translocating on DNA proximal to histone dimers. *Nat. Commun.* (2017). doi:10.1038/ncomms15616
6. J. Hong *et al.*, The catalytic subunit of the SWR1 remodeler is a histone chaperone for the H2A.Z-H2B dimer. *Mol. Cell* **53**, 498–505 (2014).
7. N. J. Krogan, *et al.*, A Snf2 Family ATPase Complex Required for Recruitment of the Histone H2A Variant Htz1. *Mol. Cell* **12**, 1565–1576 (2003).
8. Wei Yao, Sean L. Beckwith, Tina Zheng, Thomas Young, Van T. Dinh, A. Ranjan & A. J. Morrison, Assembly of the Arp5 (Actin-related Protein) Subunit Involved in Distinct INO80 Chromatin Remodeling Activities. *J. Biol. Chem.* (2015). doi:10.1074/jbc.M115.674887
9. S. Kim *et al.*, Energy transfer from an individual silica nanoparticle to graphene quantum dots and resulting enhancement of photodetector responsivity. *Sci. Rep.* **6**, 27145 (2016).
10. T. Ha, Fluorescence Resonance Energy Transfer (FRET). *Methods* **25**, 1–3 (2001).
11. R. Rahul, S. Hohng, & T. Ha, A Practical Guide to Single Molecule FRET. *Nat. Methods* **5**, 507–516 (2008).
12. D. Ray *et al.*, A compendium of RNA-binding motifs for decoding gene regulation. *Nature* **499**, 172–177 (2013).
13. Sijie Wei, Samantha J. Falk, B. E. Black and T.-H. Lee, A novel hybrid single molecule approach reveals spontaneous DNA motion in the nucleosome. *Nucleic Acids Res.* **43**, (2015).
14. H. C. Ishikawa-Ankerhold, R. Ankerhold & G. P. Drummen, Advanced fluorescence microscopy techniques-FRAP, FLIP, FLAP, FRET and FLIM. *Molecules* **17**, 4047–4132 (2012).
15. Karolin Luger, Armin W. Mäder, Robin K. Richmond, D. F. Sargent & T. J. Richmond, Crystal structure of the nucleosome core particle at 2.8 Å resolution. *Nature* **389**, 251–260 (1997).

16. Pter B. Becker, *Chromatin Protocols. Methods in Molecular Biology* **119**, (1999).
17. S. Henikoff & M. M. Smith, Histone variants and epigenetics. *Cold Spring Harb. Perspect. Biol.* **7**, 1–25 (2015).
18. Bing Li, Samantha G. Pattenden, Daeyoup Lee, Jose Gutierrez, Jie Chen, Chris Seidel, Jennifer Gerton, J. L. Workman, Preferential occupancy of histone variant H2AZ at inactive promoters influences local histone modifications and chromatin remodeling. *Proc. Natl. Acad. Sci.* **102**, 6 (2005).
19. Ryan M. Raisner, Paul D. Hartley, Marc D. Meneghini, Marie Z. Bao, C. L. Liu & Stuart L. Schreiber, Oliver J. Rando, and H. D. Madhani, Histone Variant H2A.Z Marks the 5' Ends of Both Active and Inactive Genes in Euchromatin. *Cell* **123**, 233–248 (2011).
20. H. Zhang, D. N. Roberts & B. R. Cairns, Genome-wide dynamics of Htz1, a histone H2A variant that poises repressed/basal promoters for activation through histone loss. *Cell* **123**, 219–231 (2005).
21. Benoit Guillemette, Alain R. Bataille, Nicolas Gevry, Maryse Adam, Mathieu Blanchette, F. Robert & L. Gaudreau, Variant histone H2A.Z is globally localized to the promoters of inactive yeast genes and regulates nucleosome positioning. *PLoS Biol.* **3**, 1–11 (2005).
22. C. Weber, S. Ramachandran & S. Henikoff, Nucleosomes are context-specific, H2A.Z-Modulated barriers to RNA polymerase. *Mol. Cell* **53**, 819–830 (2014).
23. Guo-Cheng Yuan, Yuen-Jong Liu, Michael F. Dion, Michael D. Slack, Lani F. Wu, Steven J. Altschuler, O. J. Rando, Genome-scale identification of nucleosome positions in *S. cerevisiae*. *Science*. **309**, 626–631 (2016).
24. I. P. Ioshikhes, I. Albert, S. J. Zanton & B. F. Pugh, Nucleosome positions predicted through comparative genomics. *Nat. Genet.* **38**, 1210–1215 (2006).
25. K. Luger, R. K. Suto, M. J. Clarkson & D. J. Tremethick, Crystal structure of a nucleosome core particle containing the variant histone H2A.Z. *Nat. Struct. Biol.* **7**, 1121–1124 (2000).
26. Jongseong Kim, Sijie Wei, Jaehyoun Lee, Hongjun Yue, and T.-H. Lee, Single-Molecule Observation Reveals Spontaneous Protein Dynamics in the Nucleosome. *J. Phys. Chem. B* 8925–8931 (2016). doi:10.1021/acs.jpcc.6b06235
27. Gaku Mizuguchi, Xuotong Shen, Joe Landry, W.-H. Wu & Subhojit Sen, C. Wu, ATP-Driven Exchange of Histone H2AZ Variant Catalyzed by SWR1 Chromatin Remodeling Complex. *Science (80-.)*. **303**, 343–348 (2004).
28. A. Ranjan *et al.*, H2A histone-fold and DNA elements in nucleosome activate SWR1-mediated H2A.Z replacement in budding yeast. *Elife* **4**, 1–11 (2015).
29. M. Papamichos-Chronakis, S. Watanabe, O. J. Rando & C. L. Peterson, Global regulation of H2A.Z localization by the INO80 chromatin-remodeling enzyme is essential for genome integrity. *Cell* **144**, 200–213 (2011).
30. A. J. Morrison & Xuotong Shen, Chromatin remodelling beyond transcription: the INO80 and SWR1 complexes. *Nat. Rev. Mol. Cell Biol.* 373–384 (2019). doi:10.1038/nrm2693

31. Blaine Bartholomew. Regulating the Chromatin Landscape: Structural and Mechanistic Perspectives. *Annu. Rev. Biochem.* 671–696 (2014). doi:10.1146/annurev-biochem-051810-093157
32. S. Watanabe & C. L. Peterson, The INO80 family of chromatin-remodeling enzymes: Regulators of histone variant dynamics. *Cold Spring Harb. Symp. Quant. Biol.* **75**, 35–42 (2010).
33. Rafael Ayala, Oliver Willhoft, Ricardo J. Aramayo, Martin Wilkinson, Elizabeth A. McCormack, Lorraine Ocloo, Dale B. Wigley, and X. Zhang, Structure and regulation of the human INO80-nucleosome complex. *Nature* **556**, 391–395 (2018).
34. Sebastian Eustermann, Kevin Schall, Dirk Kostrewa, Kristina Lakomek, Mike Strauss, Manuela Moldt, and Karl-Peter Hopfner, Structural basis for nucleosome remodeling by the INO80 complex. *Nature* **556**, 386–390 (2018).
35. V. Q. Nguyen *et al.*, Molecular architecture of the ATP-dependent chromatin-remodeling complex SWR1. *Cell* **154**, 1220–1231 (2013).
36. W. H. Wu *et al.*, Swc2 is a widely conserved H2AZ-binding module essential for ATP-dependent histone exchange. *Nat. Struct. Mol. Biol.* **12**, 1064–1071 (2005).
37. E. Luk *et al.*, Chz1, a Nuclear Chaperone for Histone H2AZ. *Mol. Cell* **25**, 357–368 (2007).
38. Z. Zhou *et al.*, NMR structure of chaperone Chz1 complexed with histones H2A.Z-H2B. *Nat. Struct. Mol. Biol.* **15**, 868–869 (2008).
39. O. Willhoft *et al.*, Structure and dynamics of the yeast SWR1-nucleosome complex. *Science* (80-.). **362**, (2018).
40. S. Watanabe *et al.*, Structural analyses of the chromatin remodelling enzymes INO80-C and SWR-C. *Nat. Commun.* **6**, 7108 (2015).
41. S. Brahma, M. Ngubo, S. Paul, M. Udugama & B. Bartholomew, The Arp8 and Arp4 module acts as a DNA sensor controlling INO80 chromatin remodeling. *Nat. Commun.* **9**, 1–10 (2018).
42. J. Y. Lee, J. Lee, H. Yue & T.-H. Lee, Dynamics of Nucleosome Assembly and Effects of DNA Methylation. *J. Biol. Chem.* **290**, 4291–4303 (2015).
43. Jaehyoun Lee, T.-H. Lee, Single-Molecule Investigations on Histone H2A-H2B Dynamics in the Nucleosome. *Biochemistry* **56**, 977–985 (2017).
44. Wei Yao, Devin A. King, Sean L. Beckwith, Graeme J. Gowans, Kuangyu Yen, Coral Zhou, A. J. Morrison, The INO80 Complex Requires the Arp5-Ies6 Subcomplex for Chromatin Remodeling and Metabolic Regulation. *Mol. Cell. Biol.* **36**, (2016).
45. Thuy T. Ngo, Q. Zhang, Ruobo Zhou, Jaya G. Yodh, and T. Ha, Asymmetric Unwrapping of Nucleosomes under Tension Directed by DNA Local Flexibility. *Cell* **160**, 1135–1144 (2015).
46. Lacramioara Bintu, Marta Kopaczynska, Courtney Hodges, Lucyna Lubkowska, Mikhail Kashlev, and C. Bustamante, The elongation rate of RNA polymerase determines the fate

of transcribed nucleosomes. *Nat. Struct. Mol. Biol.* **18**, 1394–1399 (2012).

47. Maxim Y. Sheinin, Ming Li, Mohammad Soltani, Karolin Luger, and M. D. Wang, Torque modulates nucleosome stability and facilitates H2A/H2B dimer loss. *Nat. Commun.* (2013). doi:10.1038/ncomms3579